Sensitivity of Tropical Cyclone Simulations to Parametric Uncertainties in Air–Sea Fluxes and Implications for Parameter Estimation

BENJAMIN W. GREEN AND FUQING ZHANG

Department of Meteorology, The Pennsylvania State University, University Park, Pennsylvania

(Manuscript received 26 June 2013, in final form 21 January 2014)

ABSTRACT

Tropical cyclones (TCs) are strongly influenced by fluxes of momentum and moist enthalpy across the air–sea interface. These fluxes cannot be resolved explicitly by current-generation numerical weather prediction models, and therefore must be accounted for via empirical parameterizations of surface exchange coefficients (C_D for momentum and C_k for moist enthalpy). The resultant model uncertainty is examined through hundreds of convection-permitting Weather Research and Forecasting Model (WRF) simulations of Hurricane Katrina (2005) by varying four key parameters found in commonly used parameterizations of the exchange coefficient formulas. Two of these parameters effectively act as multiplicative factors for the exchange coefficients over all wind speeds (one each for C_D and C_k); the other two parameters control the behavior of C_D at very high wind speeds (i.e., above 33 m s^{-1}). It is found that both the intensity and the structure of TCs are highly dependent upon the two multiplicative parameters. The multiplicative parameter for C_D has a considerably larger impact than the one for C_k on the relationship between maximum 10-m wind speed and minimum sea level pressure: C_D alters TC structure, with higher values shifting the radius of maximum winds inward and strengthening the low-level inflow; C_k only affects structure by uniformly strengthening/weakening the primary and secondary circulations. The TC exhibits the greatest sensitivities to the two multiplicative parameters after a few hours of model integration, suggesting that these parameters could be estimated by assimilating near-surface observations. The other two parameters are likely more difficult to estimate because the TC is only marginally sensitive to them in small areas of high wind speed.

1. Introduction

As most recently demonstrated by Hurricane Sandy (2012), tropical cyclones (TCs) have the potential to cause significant losses of life and property; minimization of these losses requires accurate forecasts of TC track, intensity, and size several days in advance. Over the past two decades, despite tremendous improvements in the prediction of TC position (track) since 1990, the ability to forecast TC intensity has stagnated (Rappaport et al. 2009). This disconnect highlights the advancements and continued limitations of numerical weather prediction (NWP) models: TC track is governed mostly by large-scale steering flows that are increasingly better resolved by global models with advanced data assimilation; TC intensity is highly sensitive to smaller-scale processes (such as fluxes across the air–sea interface) that are poorly resolved or parameterized even in regional mesoscale models. In other words, improvements to TC intensity forecasts require a reduction in the *model error* inherent to subgrid-scale parameterizations.

Large fluxes of moist enthalpy (sensible and latent heat) from the sea surface are necessary but insufficient for TC genesis, intensification, and persistence (e.g., Gray 1968). In addition to these enthalpy fluxes, momentum fluxes across the air–sea interface are believed to be crucial in determining TC intensity. For example, the well-known potential intensity (PI) theory of Emanuel (1986)—which assumes a steady-state TC in gradient and hydrostatic balance—gives analytic solutions for the maximum tangential wind speed $V_{\max}$ and minimum sea level pressure (SLP) $P_{\min}$ in nondimensional form (Emanuel 1995a,b):

$$V_{\max}^2 = \frac{C_k}{C_D}\left(\frac{1-0.25r_0^2}{1-\frac{\gamma}{2}\frac{C_k}{C_D}}\right) \quad \text{and} \tag{1}$$

Corresponding author address: Dr. Fuqing Zhang, Dept. of Meteorology, The Pennsylvania State University, 503 Walker Bldg., University Park, PA 16802.
E-mail: fzhang@psu.edu

DOI: 10.1175/MWR-D-13-00208.1

$$P_{\min} \approx -\frac{V_{\max}^2(1-0.5AH)-0.25r_0^2}{1-AH}, \qquad (2)$$

where C_k and C_D are the surface exchange coefficients of moist enthalpy and drag/momentum, respectively (see appendix A); all other variables are defined in appendix B. From (1) and (2), the ratio C_k/C_D clearly is an important factor in the pressure and wind of a *mature* storm. The sensitivity of simulated TC intensity to surface fluxes has been shown in many different studies conducted within the past half century (e.g., Ooyama 1969; Rosenthal 1971; Braun and Tao 2000; Bao et al. 2002; Bryan 2012; Green and Zhang 2013).

Unfortunately, fluxes of momentum and moist enthalpy across the air–sea interface remain poorly understood, especially for hurricane-force wind speeds; a more detailed discussion can be found in Green and Zhang (2013). Of particular importance is that C_D—once believed to increase monotonically with wind speed (e.g., Charnock 1955)—appears to saturate (e.g., Donelan et al. 2004; Black et al. 2007; French et al. 2007) or decrease (e.g., Powell et al. 2003; Jarosz et al. 2007; Holthuijsen et al. 2012) for wind speeds above $\sim$33 m s^{-1}. Observations also suggest that C_D is a function of radial distance and azimuth with respect to TC center (Vickery et al. 2009; Holthuijsen et al. 2012). Recent studies (Bao et al. 2012; Green and Zhang 2013) have found that using a saturated C_D formula affects TC structure and improves the ''pressure–wind relationship'' between $P_{\min}$ and $V_{\max}$. Interestingly, these findings appear to hold for changes to C_D over all wind speeds (i.e., not just hurricane force), a point that will be discussed in the results section. Because TC intensity and structure are strongly influenced by air–sea fluxes, the model error associated with the parameterization of these processes must be as small as possible in order to produce accurate TC forecasts.

One emerging approach toward reducing model error is the use of data assimilation. Data assimilation is a statistical method that uses observations to obtain better estimates of the initial conditions, which is crucial to producing accurate forecasts of highly nonlinear systems such as the atmosphere (Kalnay 2003). Although data assimilation is traditionally employed to estimate *state variables* for which prognostic equations exist, there is evidence that the estimation can be extended to *model parameters* for which prognostic equations do not exist (e.g., Anderson 2001; Aksoy et al. 2006a,b; Zupanski and Zupanski 2006; DelSole and Yang 2010; Hu et al. 2010; Ito et al. 2010, 2013; Peng et al. 2013; Sraj et al. 2013). Parameter estimation can be conducted in either a variational framework that requires some form of climatological error covariance or an ensemble framework that calculates error covariance directly from an ensemble of simulations. Nielsen-Gammon et al. (2010) note that model parameters are suitable for estimation in an ensemble framework if three conditions are met: *observability* (errors in observed measurements do not yield large changes in estimated parameter values), *simplicity* (model output varies smoothly with changes to the parameter), and *distinguishability* (there is a strong correlation between model parameter and state variables). We follow this outline to examine whether model parameters associated with C_D and C_k are suitable for estimation.

This particular research builds upon the work of Green and Zhang (2013), focusing on parameterized fluxes of momentum and moist enthalpy across the air–sea interface used in convection-permitting limited-area simulations of actual TCs. These flux parameterizations are quite uncertain (particularly in the strong surface winds associated with TCs) and have a substantial impact on simulated TC intensity (e.g., Green and Zhang 2013 and references therein). A battery of experiments that are similar to, but much more systematic and comprehensive than those in Green and Zhang (2013), are performed to examine the sensitivity of TC intensity and structure to parametric uncertainties in the air–sea fluxes. These sensitivity experiments also can provide useful information in identifying which set of uncertain parameters is suited for estimation. The remainder of the paper is organized as follows. Section 2 outlines the methodology of the sensitivity experiments, the results of which are shown in section 3. A general discussion can be found in section 4, followed by concluding remarks in section 5.

2. Methodology

a. Model parameters affecting C_D and C_k

A significant challenge in calculating surface fluxes is that the functional forms of the exchange coefficients for momentum C_D and moist enthalpy C_k are unknown. Thus, there are theoretically infinitely many parameters[1] that can be used to determine C_D and C_k. Consequently, it is only important that the chosen formulas (introduced below) have a *general* agreement with observations.[2]

[1] The choice of parameters to evaluate may affect the relative importance of each parameter.

[2] The danger of overfitting data by using too many parameters is highlighted in a quote attributed by Enrico Fermi to John von Neumann (Dyson 2004): ''With four parameters I can fit an elephant, and with five I can make him wiggle his trunk.''

TABLE 1. Summary of model parameters tested.

Parameter	Lower bound	Upper bound	Default value
α	0.4	1.1	1.0
V_c	$20\,\mathrm{m\,s^{-1}}$	$35\,\mathrm{m\,s^{-1}}$	$32.5\,\mathrm{m\,s^{-1}}$
m	-3.8×10^{-5}*	3.8×10^{-5}**	0.0
β	0.45	2.0	1.0

* For multiparameter experiments, the lower bound was $m = -1.9 \times 10^{-5}$ (see text).
** Sraj et al. (2013) used an upper bound of $m = 0.0$.

1) Drag coefficient

Because there is mounting evidence that there are multiple regimes (depending on wind speed and sea state) of surface drag over the ocean, it is worthwhile to investigate more than one parameter within a wind speed–dependent formula for C_D. To compare with published results, we use the three parameters estimated by Sraj et al. (2013), noting that the nonneutral stability correction is accounted for elsewhere in the surface layer code:

$$C_D = \alpha[C'_D + m \times \max(0, V - V_c)], \tag{3}$$

$$C'_D = 10^{-3}(0.692 + 0.071\tilde{V} - 0.0007\tilde{V}^2), \quad \text{and} \tag{4}$$

$$\tilde{V} = \max(2.5, \min[V, V_c]), \tag{5}$$

where V is the 10-m neutral wind speed ($\mathrm{m\,s^{-1}}$); and α, V_c, and m are the parameters to estimate (see Table 1). It should be noted that (4) and (5) originate from Kara et al. (2002) and can be found in the parameterization of the Hybrid Coordinate Ocean Model (HYCOM; Bleck 2002). Figure 1 shows the sensitivities of C_D and C_k to a range of tested parameter values.[3] Looking at (3)–(5) and Fig. 1, α controls the magnitude of C_D for all wind speeds; V_c is the critical/threshold wind speed at which C_D switches regime; and m is a highly uncertain, and likely overly simplistic, parameter that adds a linear trend to C_D only in the high-wind regime ($V \geq V_c$). Also note in Fig. 1 that changes to C_D (through α, V_c, and m) yield changes to C_k.

2) Moist enthalpy coefficient

There is an inconsistent treatment of the exchange coefficients for sensible heat C_H and latent heat C_Q (recall that moist enthalpy is the sum of sensible and latent heat) among parameterization schemes: some set $C_H = C_Q = C_k$, others have $C_H \approx C_Q \approx C_k$, and the remainder have $C_H \neq C_Q \neq C_k$ (Green and Zhang 2013). In all of the experiments of this study, C_H and C_Q are based upon the formulas used in version 3.4 of the Advanced Research Weather Research and Forecasting Model (ARW-WRF) for namelist option isftcflx = 2 (Brutsaert 1975; Garratt 1992; Green and Zhang 2013):

$$C_H = \frac{C_D}{1 + \beta^{-1} C_D^{1/2}(7.3\mathrm{Re}_*^{1/4}\mathrm{Pr}^{1/2} - 5)} \quad \text{and} \tag{6}$$

$$C_Q = \frac{C_D}{1 + \beta^{-1} C_D^{1/2}(7.3\mathrm{Re}_*^{1/4}\mathrm{Sc}^{1/2} - 5)}, \tag{7}$$

where β is an ad hoc parameter to be estimated [see Table 1 of this manuscript and Eqs. (11) and (12) of Green and Zhang (2013)]; Pr = 0.71 and Sc = 0.60 are the Prandtl and Schmidt numbers, respectively (Garratt 1992);[4] $\mathrm{Re}_* = u_* z_0/\nu$ is the roughness Reynolds number with friction velocity u_*, roughness length z_0, and kinematic viscosity of air ν; and for both (6) and (7), C_D is calculated from (3). Again, the correction for nonneutral stability is made elsewhere in the surface layer code.

From (6) and (7) and Fig. 1 of Green and Zhang (2013), it is evident that $C_H \approx C_Q$. Because air–sea fluxes of latent heat are significantly larger than those of sensible heat in TC environments (Zhang et al. 2008), it is assumed that $C_Q \approx C_k$ (and thus $C_H \approx C_k$). Also, because β does not impact C_D, β has a *first-order* effect on C_k; because C_k is a function of C_D (a consequence of similarity theory, see appendix A), the parameters α, V_c, and m have a *second-order* effect on C_k. It is, therefore, reasonable to ask if the effects of C_k can truly be separated from those of C_D given the functional forms of (6) and (7). In section 4, we show that these effects are reasonably distinguishable. The implementation of the four parameters—α, V_c, m, and β—in the numerical model sensitivity experiments is described in the next section, after an overview of the numerical model itself.

b. Experimental design

All of the sensitivity experiments used version 3.4.0 of the ARW-WRF (Skamarock et al. 2008). Because of computational constraints, only one real-data case was examined: Hurricane Katrina, a major hurricane that

[3] The WRF surface layer code calculates surface fluxes using roughness length z_0 [which can be calculated from C_D, cf. (A11)]. To prevent the code from "blowing up" during division by z_0, an additional constraint was added to keep $z_0 \geq 10^{-9}$ m, which corresponds to $C_D > 0.3 \times 10^{-3}$. The smallest drag coefficient given in the literature for an intense hurricane is $C_D = 0.7 \times 10^{-3}$ for wind speeds of $60\,\mathrm{m\,s^{-1}}$ [p. 7 of Holthuijsen et al. (2012)].

[4] Any of the parameters in (6) and (7), such as Pr and Sc, can be estimated. Offline tests (not shown) reveal that C_H and C_Q are more sensitive to β than to Pr or Sc.

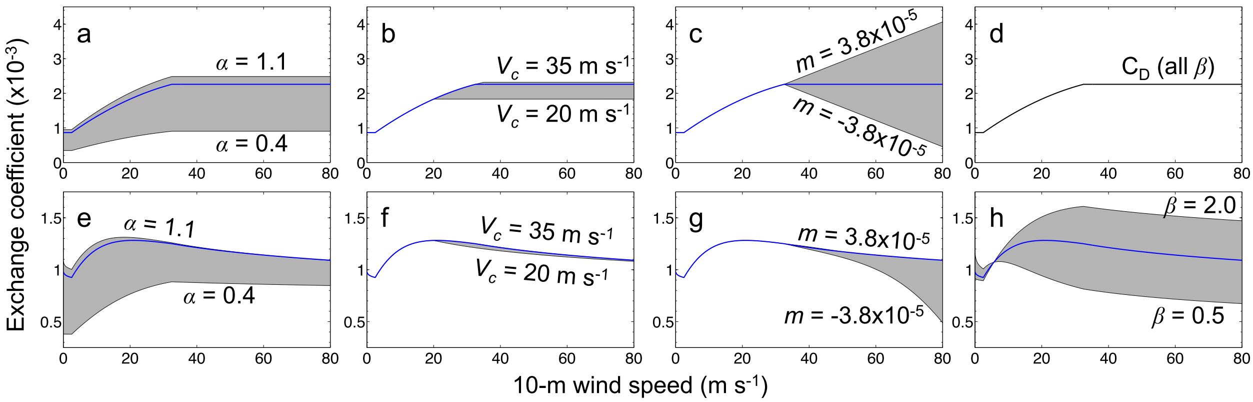

FIG. 1. Plots of (top) C_D and (bottom) C_k [technically C_Q from (7), see text for discussion] as functions of 10-m wind speed for the single-parameter experiments (see Table 1) that varied (a),(e) α; (b),(f) V_c; (c),(g) m; and (d),(h) β. Each shaded area represents the possible range of exchange coefficients given the allowed range of parameter values; the labeled edge lines show the exchange coefficient curves given by the minimum and maximum allowed parameter values. Blue lines denote exchange coefficient curves for the default value of the varied parameter (cf. last column in Table 1).

tracked across the Gulf of Mexico in late August 2005 (Knabb et al. 2006). With the exception of the parameterizations for C_D and C_k, the simulations were configured identical to Green and Zhang (2013); for completeness, the details of the model setup are repeated here.

There were three domains—D01, D02, and D03 (results are from D03 unless otherwise stated)—with horizontal grid spacings of 27, 9, and 3 km, respectively (all domains used 43 vertical levels); the corresponding time steps were 60, 20, and 20/3 s. Convection was explicitly resolved in D02 and D03, and parameterized in D01 via the Grell–Devenyi cumulus scheme (Grell and Devenyi 2002). Radiation was parameterized by the Rapid Radiative Transfer Model for longwave (Mlawer et al. 1997) and the Dudhia (1989) scheme for shortwave. Cloud microphysics were represented by the WRF single-moment 6-class (with graupel) scheme (Hong and Lim 2006), and the Yonsei University (YSU) planetary boundary layer scheme (Hong et al. 2006) was used with "MM5 similarity" (sf_sfclay_physics option 1) and five-layer thermal diffusion over land. For all of the experiments, single-column (1D) ocean mixing (Pollard et al. 1972) was turned off to isolate the effects of exchange coefficient parameterizations.

There are two distinct components to the experimental procedure. The first is an assimilation stage identical to that of Green and Zhang (2013), which can be summarized as follows. To start, a 60-member ensemble was initialized at 0000 UTC 25 August 2005 by adding perturbations to Global Forecast System (GFS) initial conditions (ICs) and lateral boundary conditions (LBCs); the ensemble was integrated forward until 1430 UTC to generate a flow-dependent error covariance matrix. Then, six rounds of airborne Doppler radar velocity data were assimilated between 1430 and 2000 UTC using the ensemble Kalman filter (EnKF) data assimilation technique (Zhang et al. 2009; Weng and Zhang 2012). Last, the posterior mean of the 60-member ensemble at 2000 UTC was integrated forward an additional 4 hours to 0000 UTC 26 August 2005. It should be noted that in this first 24-h period, the domains were fixed in space and the surface fluxes were parameterized using the WRF namelist option isftcflx = 2 *as formulated in version 3.4.0.*[5]

The second component of the experimental procedure is the sensitivity stage, during which numerous simulations were run with the same ICs and LBCs but with slightly different parameterizations of C_D and C_k. To examine parameter sensitivity as a function of initial TC intensity, two different start times were used: 0000 UTC 26 August and 0000 UTC 27 August, although the end time was the same for both (0000 UTC 31 August). For each start time, two sets of experiments were run (as in Nielsen-Gammon et al. 2010): single parameter (one parameter varied at a time) and multiparameter (all parameters varied simultaneously).

1) SINGLE-PARAMETER EXPERIMENTS

The single-parameter experiments—used to determine parameter observability (Nielsen-Gammon et al. 2010)—can also be thought of as four independent

[5] The reasons for this are detailed in Green and Zhang (2013). For the purposes of the present research, it is only important that the surface flux parameterizations be consistent *in the sensitivity stage*.

experiments, one for each parameter. Let $\mathbf{\Psi}^k$ be an arbitrary model parameter such that $\Psi^1 = \alpha$, $\Psi^2 = V_c$, $\Psi^3 = m$, and $\Psi^4 = \beta$. For each $\mathbf{\Psi}^k$, 20 different values $\mathbf{\Psi}^k_{x=1,2,\ldots,20}$ are generated at equally spaced intervals within the allowed range of parameter values (e.g., $\Psi^1_1 = \alpha_{\min} = 0.4$ and $\Psi^1_{20} = \alpha_{\max} = 1.1$). Additionally, the three parameters not being varied are fixed at their default values given in Table 1: for example, when $\mathbf{\Psi}^{k=1}$ (i.e., the sensitivity to α is being tested), then $V_c = 32.5\,\mathrm{m\,s^{-1}}$, $m = 0$, and $\beta = 1$. A total of 160 (20 parameter values for each of 4 parameters for each of 2 start times) single-parameter simulations were run. One concern was with the range of m values: looking at Fig. 1c, large negative values of m yield C_D values less than 0.5×10^{-3} (cf. footnote 3). Therefore, for the multiparameter experiments, the lower limit of m was revised to $m = -1.9 \times 10^{-5}$.

2) Multiparameter experiments

Parameter distinguishability is ascertained from multiparameter experiments (Nielsen-Gammon et al. 2010). Here, as in the single-parameter experiments, each parameter $\mathbf{\Psi}^k$ can have one of 20 possible values (as stated above, the multiparameter experiments have a smaller range of m values). Unfortunately, testing the entire parameter space (i.e., all $20^4 = 160\,000$ possible combinations of α, V_c, m, and β) is computationally prohibitive. Instead, 80 different rows of the $160\,000 \times 4$ parameter matrix $\begin{bmatrix} \Psi^1_1 & \cdots & \Psi^4_1 \\ \vdots & \ddots & \vdots \\ \Psi^1_{20} & \cdots & \Psi^4_{20} \end{bmatrix}$ were selected at random from a uniform distribution (i.e., each row had an equal likelihood of being selected); then, 80 different simulations (one for each set of parameter values) were run. The same 80 sets of parameter values were used for both start times (0000 UTC 26 and 27 August) for a total of 160 multiparameter simulations. The results shown below are from the 320 successful simulations (160 single parameter and 160 multiparameter).

3. Sensitivity of TC intensity and structure to realistic parameter uncertainties

a. TC intensity

As is evident in Fig. 1, changes to the different model parameters have varying degrees of influence on C_D and C_k; therefore, it would be expected that the different model parameters have varying degrees of influence on TC intensity (in terms of both maximum 10-m wind speed and minimum SLP). Figures 2 and 3, which show hourly output from the multiparameter sensitivity experiments initialized at 0000 UTC 26 August (Fig. 3 also shows experiments initialized at 0000 UTC 27 August), are consistent with such an expectation. For example, changes to V_c only marginally affect the exchange coefficients at strong surface wind speeds and consequently have a minimal impact on TC intensity (as indicated by the absence of statistically significant correlations in Fig. 3). At the other extreme, both C_k and TC intensity are highly sensitive to β, although this parameter does not appear to noticeably change the pressure–wind relationship; note that increasing β (increasing C_k) yields a stronger TC in terms of both pressure (correlation coefficients approaching -1 by the time of landfall) and wind (correlations greater than 0.4 after 1–2 days). The two parameters with the greatest impact on C_D (α and m) also considerably impact TC intensity. Moreover, consistent with prior results (Bao et al. 2012; Green and Zhang 2013), changes to surface momentum flux change the pressure–wind relationship of the TC; that said, α and m change the pressure–wind relationship in significantly different ways. The parameter m (which only impacts C_D for wind speeds at or above V_c) has statistically significant correlations with maximum 10-m wind speed (larger m means larger C_D and thus weaker 10-m winds) but not with minimum SLP. Changes to α (which impacts C_D and C_k over all wind speeds) yield statistically significant correlations with both intensity metrics, but the pressure–wind relationship is clearly changed because increasing α yields TCs with weaker winds (correlations close to -1 during the first few hours) but with substantially lower minimum SLP (correlations more negative than -0.4 until just before landfall).

Figures 2 and 3 can also be used to identify *simple* parameters (for future parameter estimation), which ideally have a linear relationship with the various state variables. Because the curves in Fig. 2 are colored according to parameter value (from low values in blue to high values in red), simple parameters will have intensity curves that progress in a rainbow-like manner (i.e., the colors appear ''sorted'' rather than jumbled). For example, β is a simple parameter for both intensity metrics. Simplicity is evident for α with the exception of 10-m wind speed between approximately 6 and 72 h; this exception is almost certainly a consequence of α changing the pressure–wind relationship. Similarly, m has a simple relationship with 10-m wind speed but only after the TC has strong enough wind speeds over a sufficiently large area (recall that m only matters for wind speeds above V_c). It is difficult to assess the simplicity of V_c because changes to this parameter have little effect on TC intensity (in terms of both minimum SLP and maximum 10-m wind speed) throughout the simulation period. Figure 3 is consistent with Fig. 2 in that the

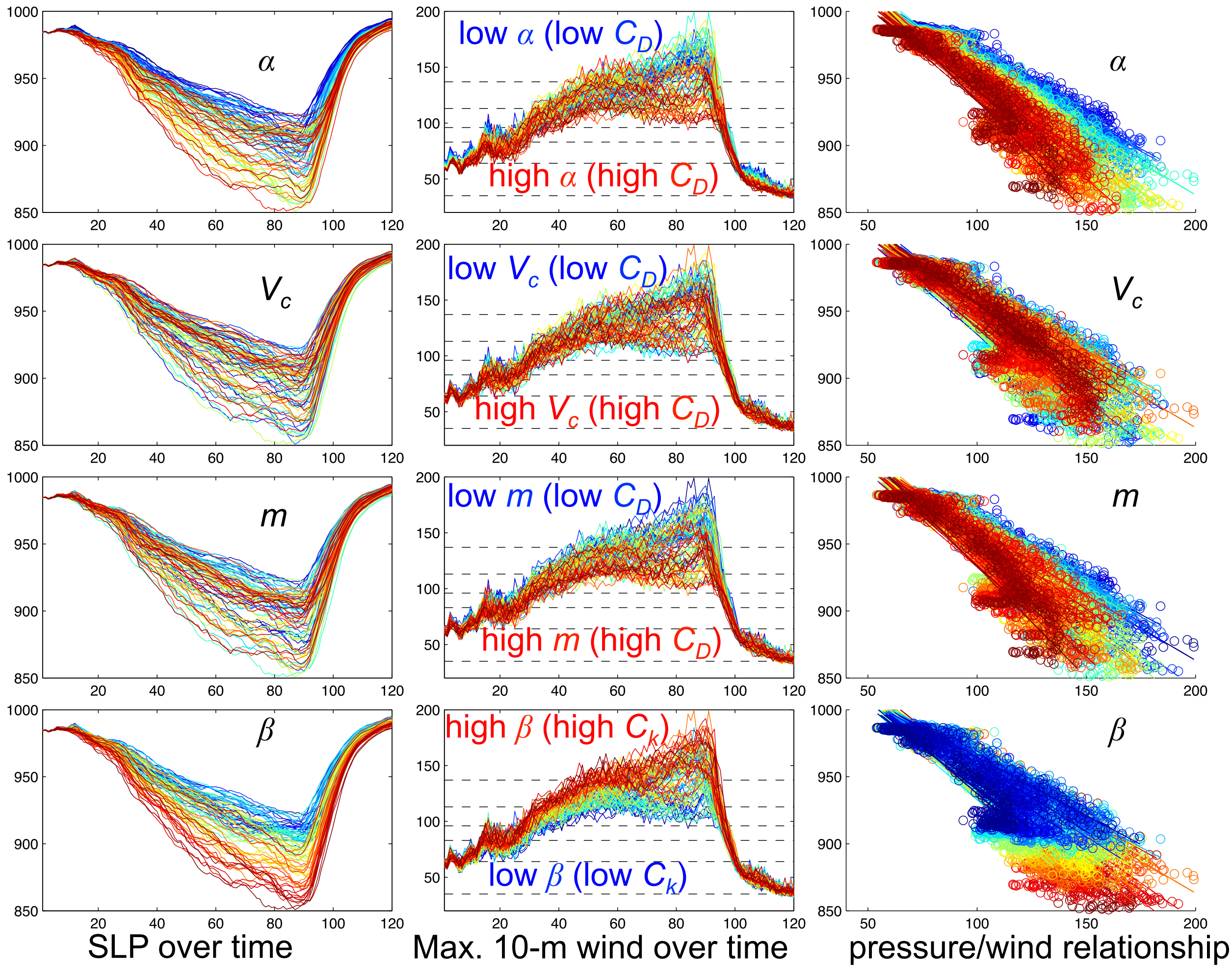

FIG. 2. Results from hourly output of the 80 multiparameter simulations initialized at 0000 UTC 26 Aug 2005. (from top to bottom) Rows show the sensitivity of TC intensity to model parameters α, V_c, m, and β (as indicated). Time series of (left) minimum SLP (hPa) and (middle) maximum 10-m wind speed (kt, 1 kt = 0.5144 m s^{-1}; dashed lines denote Saffir–Simpson hurricane wind scale intensities) are given. (right) The relationship between minimum SLP and maximum 10-m wind speed (open circles mark hourly output; lines of best fit also shown) during the first 91 h of the simulation (later times were omitted to remove the impact of landfall). Colors represent the individual simulations, for parameter values ranging from the lowest tested value (dark blue) to the highest tested value (dark red).

simple (linear) parameters have statistically significant linear correlation coefficients with TC intensity. The single-parameter experiments were in agreement with the multiparameter experiments in terms of simplicity (not shown).

Beyond this point, we will focus on the effects of α and β. From Figs. 1–3, it is clear that V_c has only minor impacts not just on C_D and C_k, but also on minimum central pressure and maximum 10-m wind speed. Parameter m can have large impacts (particularly on C_D; Fig. 1c), but only for winds of hurricane force, including the eyewall. Obviously, eyewall processes are crucial for TC structure and intensity regardless of size. That said, successful estimation for a parameter such as m requires a storm with strong enough winds (i.e., greater than V_c) over a large enough area (such that the covariance has a large sample size), which is not the case for weaker TCs.

b. Azimuthally averaged TC structure

Thus far, the effects of the parameters on the simulated TCs have only been examined in terms of the "point metrics" of intensity (minimum SLP and maximum 10-m wind speed). Particularly for parameters that change the pressure–wind relationship, it is worthwhile to look at the spatial correlations (i.e., structural changes) of the parameters. Figure 4 shows the correlations between α and azimuthally averaged fields of SLP and 10-m wind speed as a function of time and radial distance from TC center for multiparameter experiments initialized at both start times; the ensemble

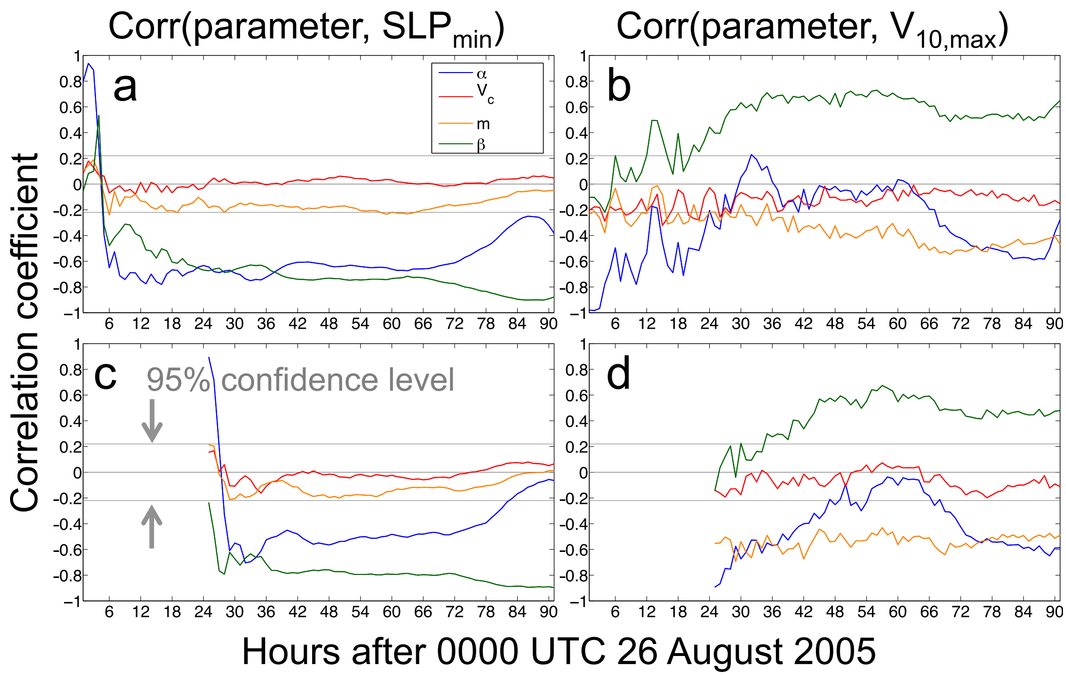

FIG. 3. (a) Time series plots of correlation coefficients between model parameters (α in blue, V_c in red, m in orange, and β in green) and minimum SLP for multiparameter experiments initialized at 0000 UTC 26 Aug 2005. (b) As in (a), but for correlations between model parameters and maximum 10-m wind speed. (c),(d) As in (a),(b), but for simulations initialized at 0000 UTC 27 Aug 2005. Correlation values of ± 0.22 are marked to denote the 95% level for statistical significance; the zero correlation line is also drawn. Hourly output is restricted to times before 2000 UTC 29 Aug 2005 to remove the effects of landfall.

mean 10-m wind field is contoured for reference. There are several striking features. After the simulated TCs have intensified to hurricane strength, the effect of α on the structure of the wind field is clear: larger α (larger C_D for all wind speeds) results in a radius of maximum wind (RMW) that is closer to the center, as indicated by the *increase* in the 10-m wind inside the ensemble mean RMW. As expected, larger α also weakens winds for all locations outside the RMW. Throughout much of the TC over nearly all times, the magnitude of the correlation coefficient exceeds 0.8, a testament to the importance of α for low-level wind speeds. The relationship between α and the azimuthally averaged SLP is somewhat less straightforward. In the far field (beyond 150 km from center), larger α yields a lower pressure, possibly because of the increase in C_k. Near and just inside the RMW, there is a dipole pattern in the pressure correlation such that larger α leads to a steeper radial SLP gradient and deeper central pressure; this is in agreement with recent findings [cf. Fig. 6 in Green and Zhang (2013)]. There is also a notable temporal variation in the correlation between α and SLP: in the first few hours of model integration, increasing α yields higher pressure at the TC center, which suggests that the impact of C_D on central pressure is a not a direct effect but rather a consequence of the changed vortex structure (i.e., size of RMW) and the degree of high-enthalpy inflow from the far field. Figure 5 is identical to Fig. 4 except that correlations with β are shown instead. Not surprisingly, an increase in β (increase in C_k) leads to lower SLP throughout the entire TC (rather than just inside the RMW). Additionally, an increase in C_k is strongly correlated with an increase in 10-m wind speed at the RMW (with a weaker, but still statistically significant, correlation at farther distances). The lack of a dipole pattern means that β (and thus C_k) does not impact TC structure in the same way as C_D. There is some temporal dependence on the correlations with β, most likely because the TC increases in size over time.

The effects of the parameters (viz., α and β) on TC structure can also be examined via radius–height plots of correlations with azimuthally averaged tangential and radial winds and equivalent potential temperature θ_e. Such plots are shown in Figs. 6–8 for multiparameter simulations initialized at 0000 UTC 27 August and valid 1, 24, and 48 h later, respectively. After just 1 h (Fig. 6), there are two coherent correlation features: one is between α and low-level wind such that increasing α (and thus C_D) yields more surface friction, which as expected slows the tangential winds (Fig. 6a) and strengthens the

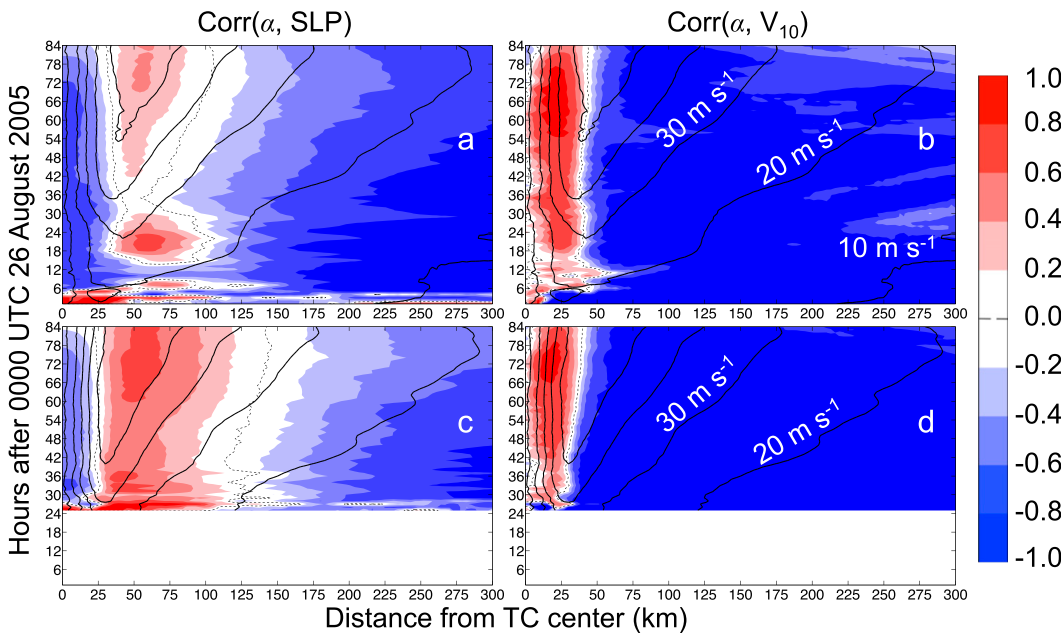

FIG. 4. (a) Correlations (color shading) between model parameter α and azimuthally averaged SLP as functions of distance from TC center and hours after 0000 UTC 26 Aug 2005 for multiparameter simulations initialized at 0000 UTC 26 Aug 2005. (b) As in (a), but for correlations between α and azimuthally averaged 10-m wind speed. (c),(d) As in (a),(b), but for simulations initialized at 0000 UTC 27 Aug 2005. The thin dashed lines denote the contour of zero correlation; the heavy black lines denote the ensemble mean (over all 80 simulations) azimuthally averaged 10-m wind speed.

low-level inflow (Fig. 6c). The second coherent feature is the positive correlation near the surface between θ_e and both parameters (Figs. 6e,f), which is to be expected because increases to α and β yield increased C_k (the former through an increase in C_D) and thus increased surface fluxes of sensible and latent heat. Unsurprisingly, these results suggest that estimating parameters associated with C_D and C_k would best be accomplished with observations as close to the surface as possible. At 24 and 48 h (Figs. 7 and 8), the correlation structures

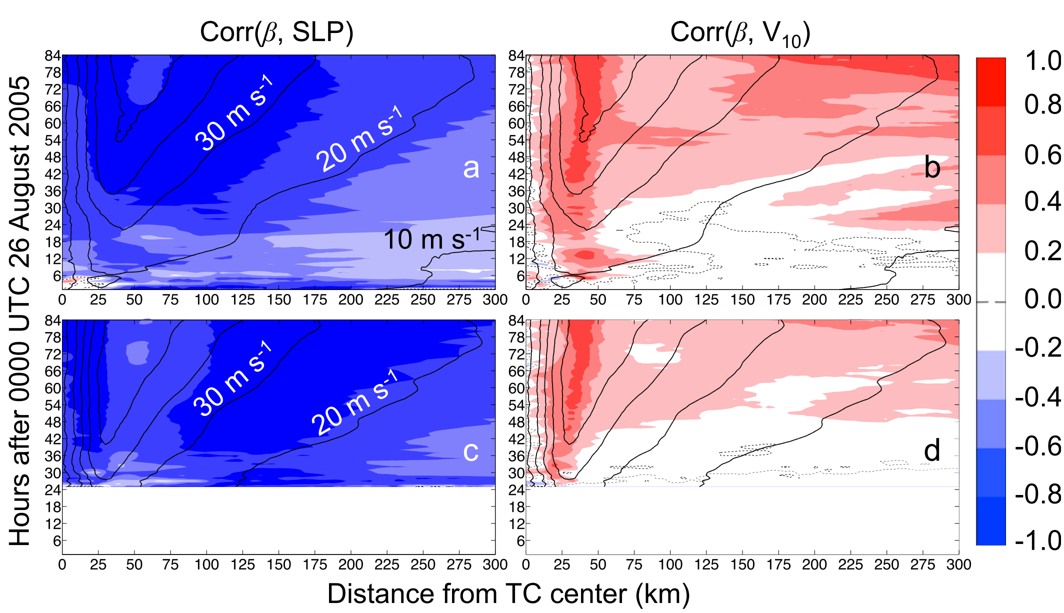

FIG. 5. As in Fig. 4, but for correlations with model parameter β.

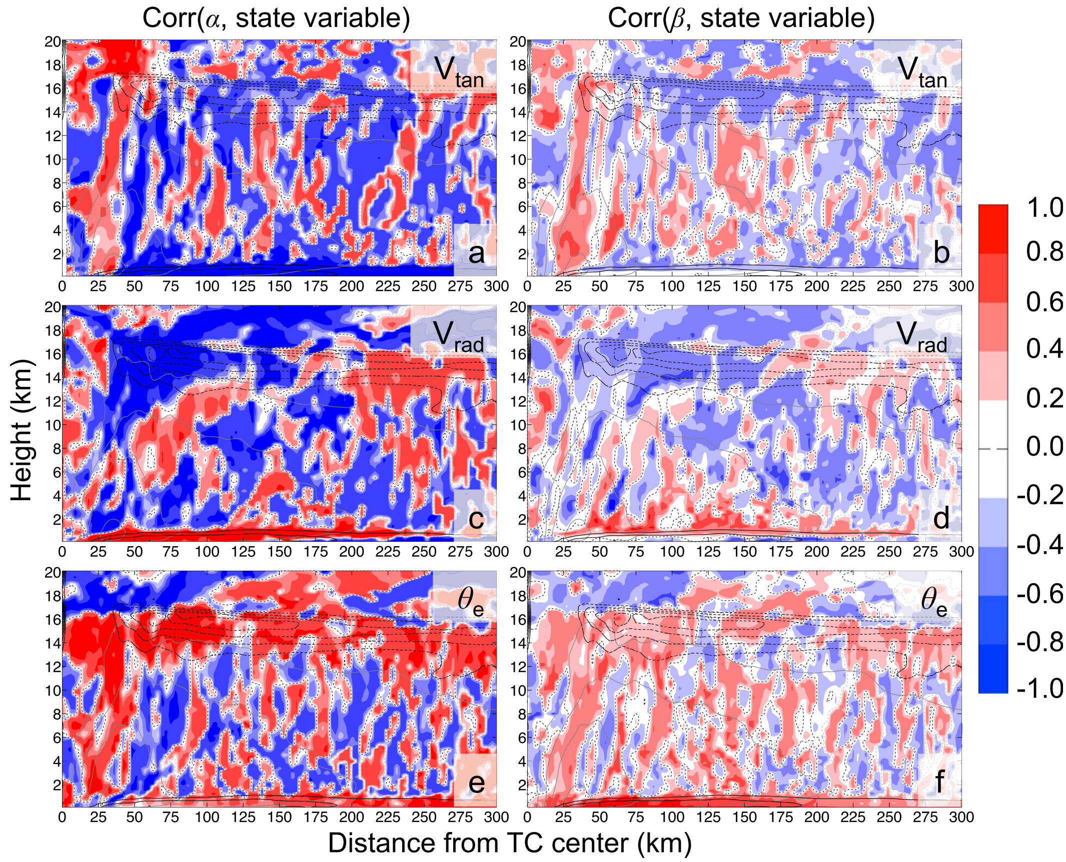

FIG. 6. Radius–height plots for multiparameter experiments initialized at 0000 UTC 27 Aug 2005, valid at 0100 UTC 27 Aug 2005. (a) Correlation coefficients (color shading) between α and azimuthally averaged tangential wind. (b) As in (a), but for correlations between β and tangential wind. (c),(d) As in (a),(b), but for correlations with radial wind (positive values denote *inflow*). (e),(f) As in (a),(b), but for correlations with equivalent potential temperature. The wind field averaged over all 80 simulations is shown in each plot, with solid gray contours denoting tangential wind (every 10 m s^{-1}), and heavy solid (dashed) black contours denoting radial inflow (outflow) every 3 m s^{-1}. The thin dashed lines denote the contour of zero correlation.

become considerably smoother, which allows for insights into physical/structural processes in a more comprehensive manner than Green and Zhang (2013, cf. their Fig. 7). Above the low-level inflow layer (where increasing α yields stronger inflow at the expense of the tangential wind and a smaller radius of maximum winds), increased α results in a tighter vortex (mainly inside ~175 km) and stronger upper-level outflow. The correlations with β are consistent with the idea that this parameter governs TCs in a much simpler way: increasing β (increasing C_k) yields a more intense vortex, with faster tangential winds throughout the free atmosphere, a stronger secondary circulation, and an across-the-board increase in θ_e; the radius of maximum winds does not shift. Furthermore, the eyewall is the only region where the strong correlation between tangential wind (which is much larger than the radial wind) and β reaches into the boundary layer down toward the surface; this explains the weaker correlations beyond ~75 km from TC center between β and 10-m wind speed shown in Fig. 5.

It is worth noting that there are apparent downward and outward phase propagations of correlation bands with alternating sign for both parameters in the wind fields and in θ_e (in particular during the first 24 h, not shown). These bands are likely induced by inertial gravity waves radiating away from the eyewall/outflow regions as an adjustment and reflection of TC intensity changes under different air–sea fluxes. The detailed understanding of such processes is beyond the scope of the current study.

c. Three-dimensional sensitivity

It is also worthwhile to examine correlations between model parameters and state variables without azimuthal averaging, because neither TCs nor their observations

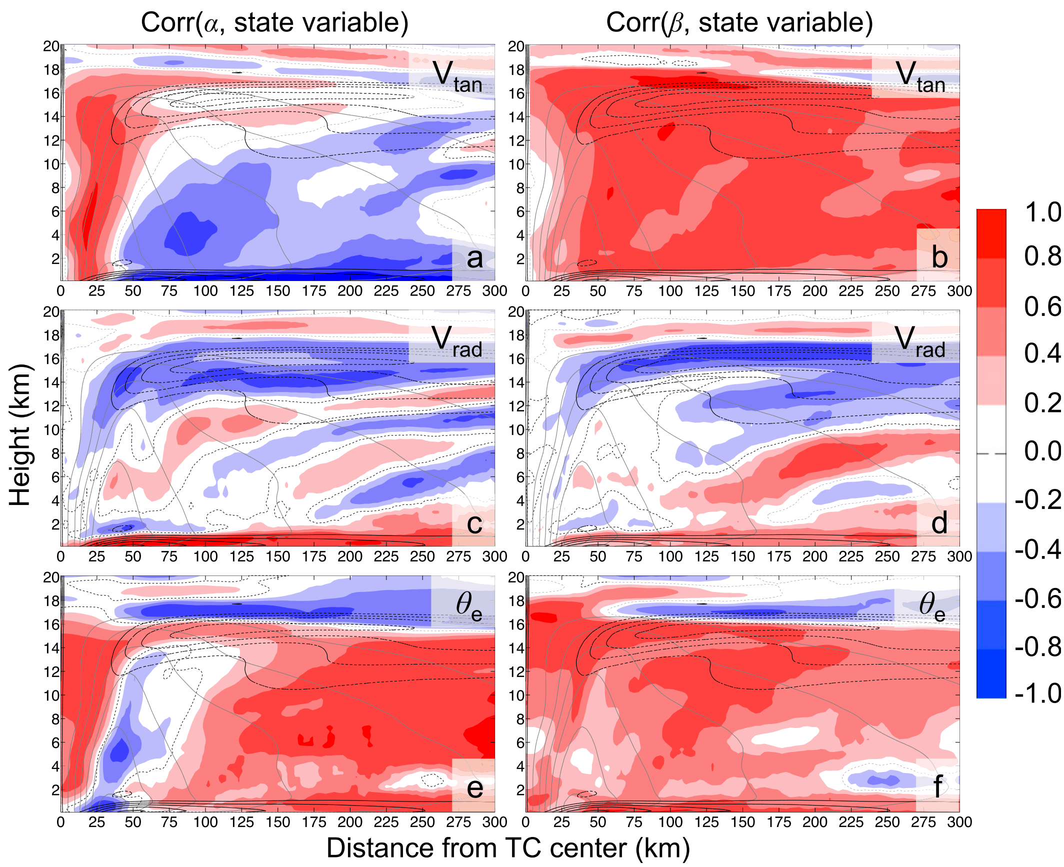

FIG. 7. As in Fig. 6, but valid at 0000 UTC 28 Aug 2005.

are axisymmetric. In doing so, we focus on the lowest model level (with a height of ~35 m) as a proxy for the surface because near-surface observations are likely to be the most beneficial for parameter estimation. Figures 9 and 10 show multiparameter experiment correlations between (α, β) and lowest model level wind speed after 1 and 12 h of model integration, respectively. These correlations are shown in an Earth-relative framework, which is often used for data assimilation in real cases. There are statistically significant correlations (indicating parameter *distinguishability*) between α and wind speed throughout the shown portion of D03 after just 1 h of integration (Fig. 9), which is to be expected by the definition of α. Over almost the entire shown part of the domain, increasing α (and thus C_D) yields lower near-surface winds over the ocean. On the other hand, there are no large areas of statistically significant correlations with β—in fact, most of the statistically significant correlations are over *land*—demonstrating that near-surface wind speed observations may not be able to help estimate this parameter with extremely short-term model integration and data assimilation. Looking to 12 h after model initialization (Fig. 10), which is on the order of the time needed to spin up covariance structures in an ensemble data assimilation system, there are areas of statistically significant correlations for both parameters. Such a result suggests that while near-surface wind speed observations, especially near the TC center, can always be helpful in estimating α, a longer spinup time may be needed for such observations to have an impact on β (consistent with the findings from azimuthally averaged fields). It should also be noted that after 12 h of integration, the impact of α on the vortex structure is already apparent (especially for the simulations initialized at 0000 UTC 27 August; Fig. 10b): increasing α increases the wind close to the vortex center and decreases the wind at larger radii, a pattern that is consistent with a decrease in the radius of maximum wind (see, e.g., Fig. 5a of Smith et al. 2013).

Asymmetric correlations at later times may be able to provide additional insights into physical processes, although these correlations must be shown in a vortex-centered framework to remove the effects of different forward motion vectors. By 25 h after model initialization (Fig. 11), correlations between α and lowest model level wind speed are mostly dominated by the

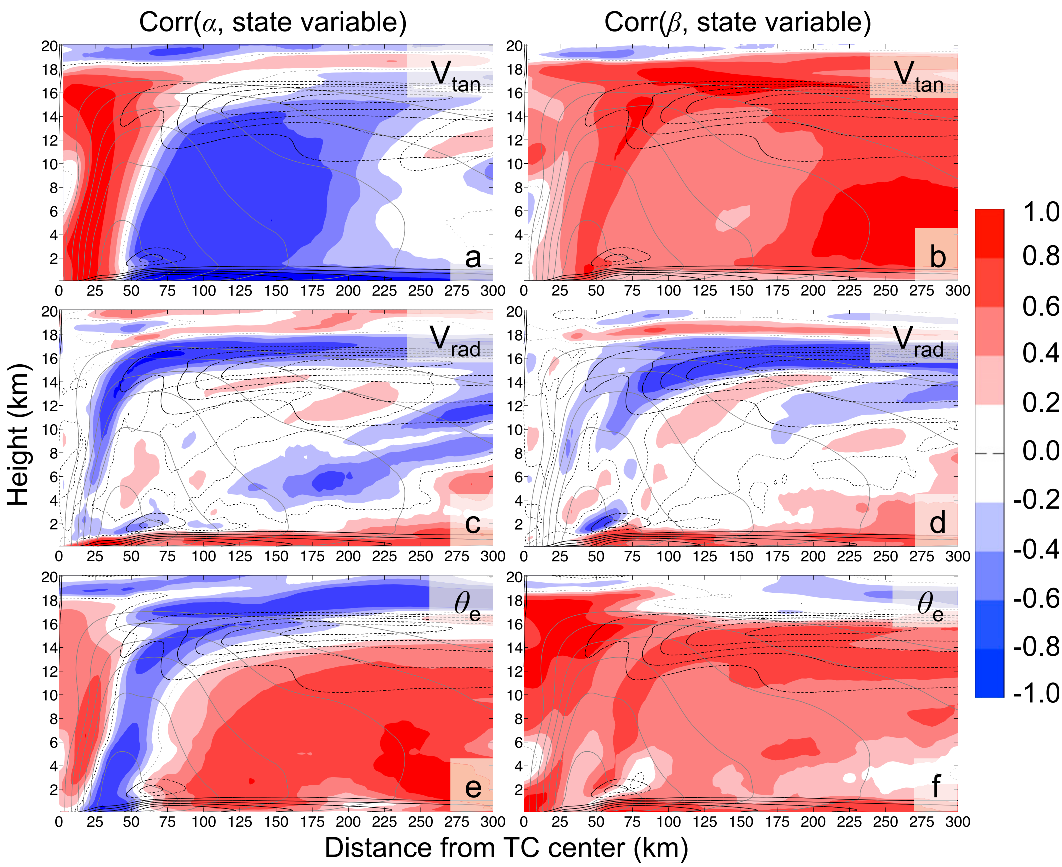

FIG. 8. As in Fig. 6, but valid at 0000 UTC 29 Aug 2005.

wavenumber-0 structure and consistent with the azimuthally averaged results (e.g., Figs. 4, 5, and 7), with increasing α (increasing C_D) shrinking the near-surface RMW and weakening winds beyond the RMW. The only deviation from this pattern is a consequence of landmasses (Florida and Cuba, especially in Fig. 11a). Correlations with β, however, exhibit substantial azimuthal and radial variability that cannot be attributed to nearby land; this is true even for winds close to airborne Doppler flight level (~2 km, not shown). It is possible that the asymmetries are a consequence of β only affecting winds near the eyewall, but this is purely speculation.

Finally, parameters to be estimated must yield sufficiently large spread in the state variables, which Nielsen-Gammon et al. (2010) call *observability*. It should be noted that the temporal evolution of standard deviation depends greatly on the atmospheric state: standard deviations will grow monotonically in environments that are sensitive to the initial conditions (such as an intensifying TC), but not necessarily so in environments that are highly forced by boundary conditions (such as the diurnal cycle under large-scale quiescent conditions).

Figure 12 shows the standard deviation of the lowest model level wind speed for *single-parameter* experiments[6] after a single hour of model integration. Several important points are evident from this figure. First, standard deviations for both parameters are an order of magnitude larger for the later start time (0000 UTC 27 August; Figs. 12b,d), presumably because the stronger TCs at this later time result in more significant changes to the exchange coefficients (note that the spread of C_D and C_k increases with wind speed in Fig. 1). Second, the standard deviations associated with α are more than an order of magnitude larger than those for β (and for V_c and m, not shown). Third, the standard deviations exhibit substantial spatial variability, such that the largest standard deviations are collocated with the fastest winds. While this is to be expected (small changes in position or TC size could yield large differences in wind speed at a fixed point on Earth), there are major implications for TC prediction. From the

[6] The standard deviations from multiparameter experiments cannot be separated into contributions from individual parameters.

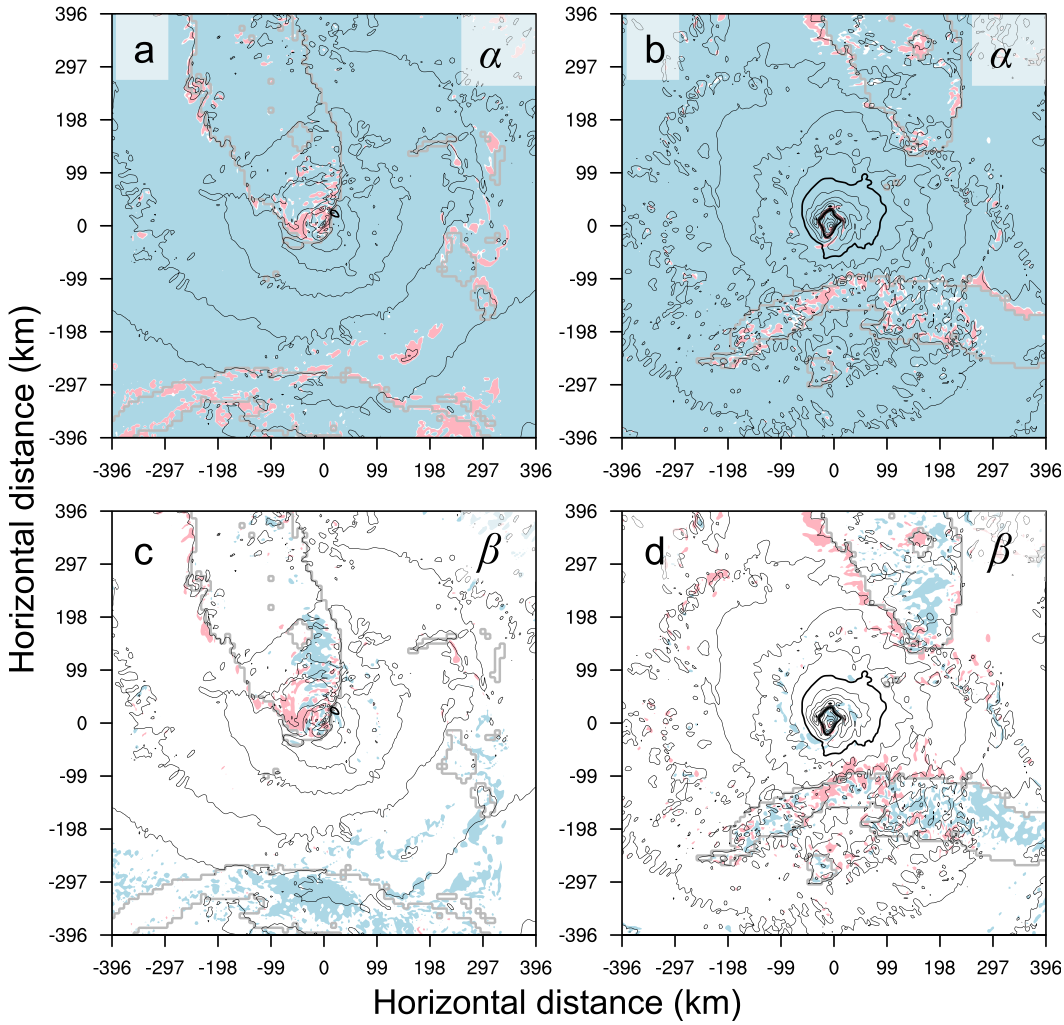

FIG. 9. Earth-centered output (coastlines in gray) from multiparameter experiments valid 1 h after initialization at (left) 0000 UTC 26 Aug and (right) 0000 UTC 27 Aug 2005. Lowest model level (~35 m above ground level) wind speed averaged over all multiparameter experiments is contoured every 5 m s^{-1} (heavy contours denote 30 and 60 m s^{-1} isotachs). Red (blue) shading indicates positive (negative) statistically significant correlations (at the 95% level) between lowest model level wind speed and model parameters (a),(b) α and (c),(d) β. Axis labels denote distance in km from a fixed point close to the average TC center.

standpoint of observability (large standard deviations), the observations most suitable for use in parameter estimation would be taken near the TC center and over the open ocean, which is in line with the current practice for airborne reconnaissance. In terms of TC predictability, it is crucial to accurately resolve the structure of the inner vortex because that is the location of the largest (and thus fastest growing) errors.

4. Discussion

Any case study will raise questions about the robustness of the results. Perhaps one of the most obvious questions is whether or not the findings translate well to other TCs. Obviously, the best way to answer this question would be to run an additional 320+ high-resolution simulations but for a completely different TC; computational and data storage constraints make this unfeasible. A related concern is that the parameter space for the multiparameter experiments is quite undersampled, in terms of both the fraction of parameter combinations selected (80/160 000 = 0.05%) and the method used to sample the parameter space [a Latin Hypercube could have been used instead of or in addition to the uniform random distribution employed here, see chapter 2 of Saltelli et al. (2008) for an excellent overview]. Nevertheless, our results are consistent with previously published studies. For instance, both Bao

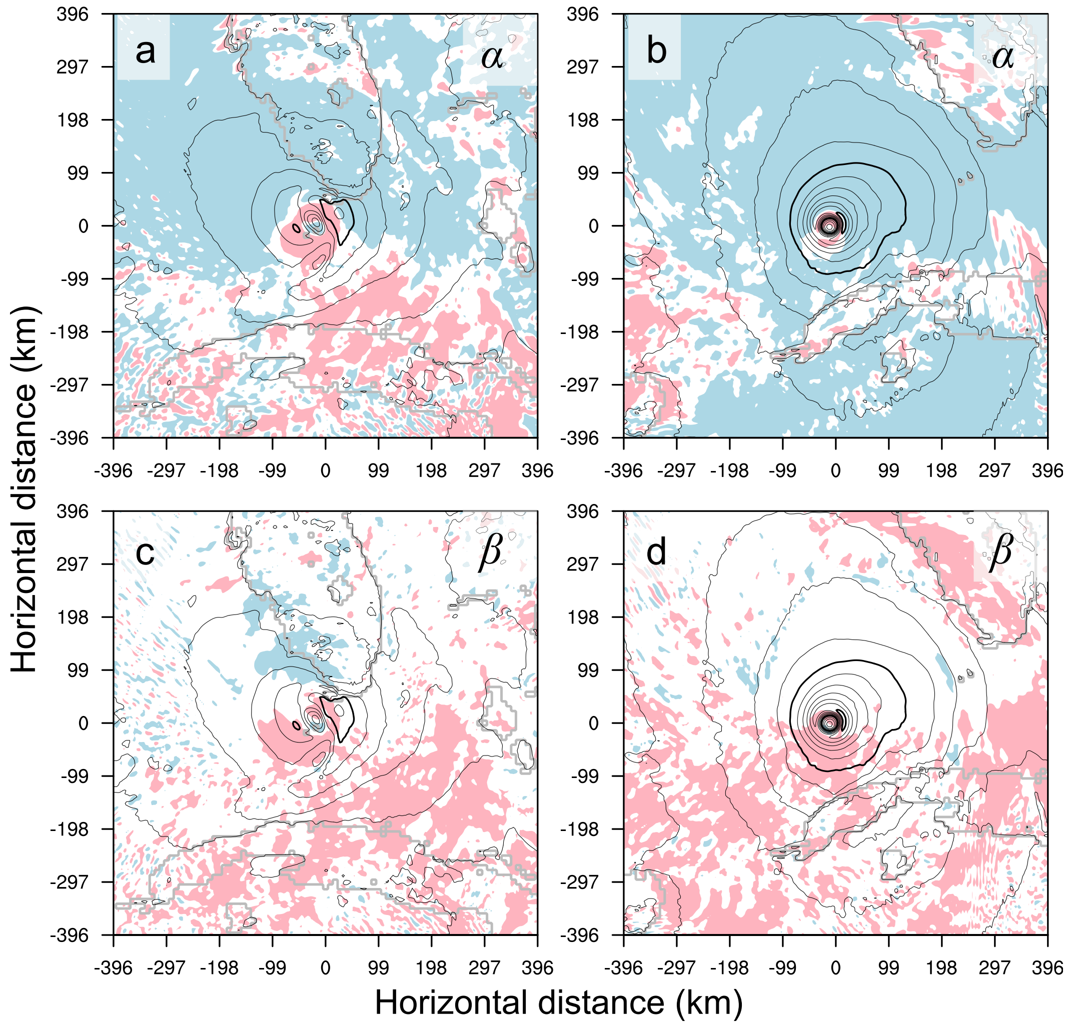

FIG. 10. As in Fig. 9, but valid 12 h after initialization.

et al. (2012) and Green and Zhang (2013) found that C_D impacts the pressure–wind relationship of the TC; in fact, Green and Zhang (2013) showed this result to hold across several different cases (cf. their Fig. 9). These two studies also found C_D to affect TC structure, including the radius of maximum winds.

The identification of model parameters suitable for estimation also has support from previous work. Specifically, Sraj et al. (2013) used Bayesian inference to estimate α, V_c, and m for a simulation of Typhoon Fanapi (2010).[7] Their method was quite confident (although not necessarily accurate) in its estimate of α, with a small-variance Gaussian posterior distribution; the estimate of m, however, had a nearly uniform posterior distribution, indicating low confidence. Although Sraj et al. (2013) used a different estimation method than what is planned for our future work, the fact that α seems to be a good parameter to estimate is consistent with the present results. Interestingly, their estimate of V_c was of reasonable confidence, which is in disagreement with our parameter sensitivity experiments (a more comprehensive discussion is beyond the scope of this paper). Regarding m, Sraj et al. (2013) note that their observational dataset did not include locations at which wind speeds rose above V_c (i.e., wind speeds for which m would matter); consequently, their algorithm was unable to provide an improved estimate of m. This problem underscores one of the reasons why we believe that m, while important for TC dynamics, is not a suitable parameter to estimate: m only matters for very strong winds (hurricane force, or above V_c) that are almost always confined to a small area or, in the case of

[7] Note that in Sraj et al. (2013), V_c is called V_{max} and the upper bound for m is 0.

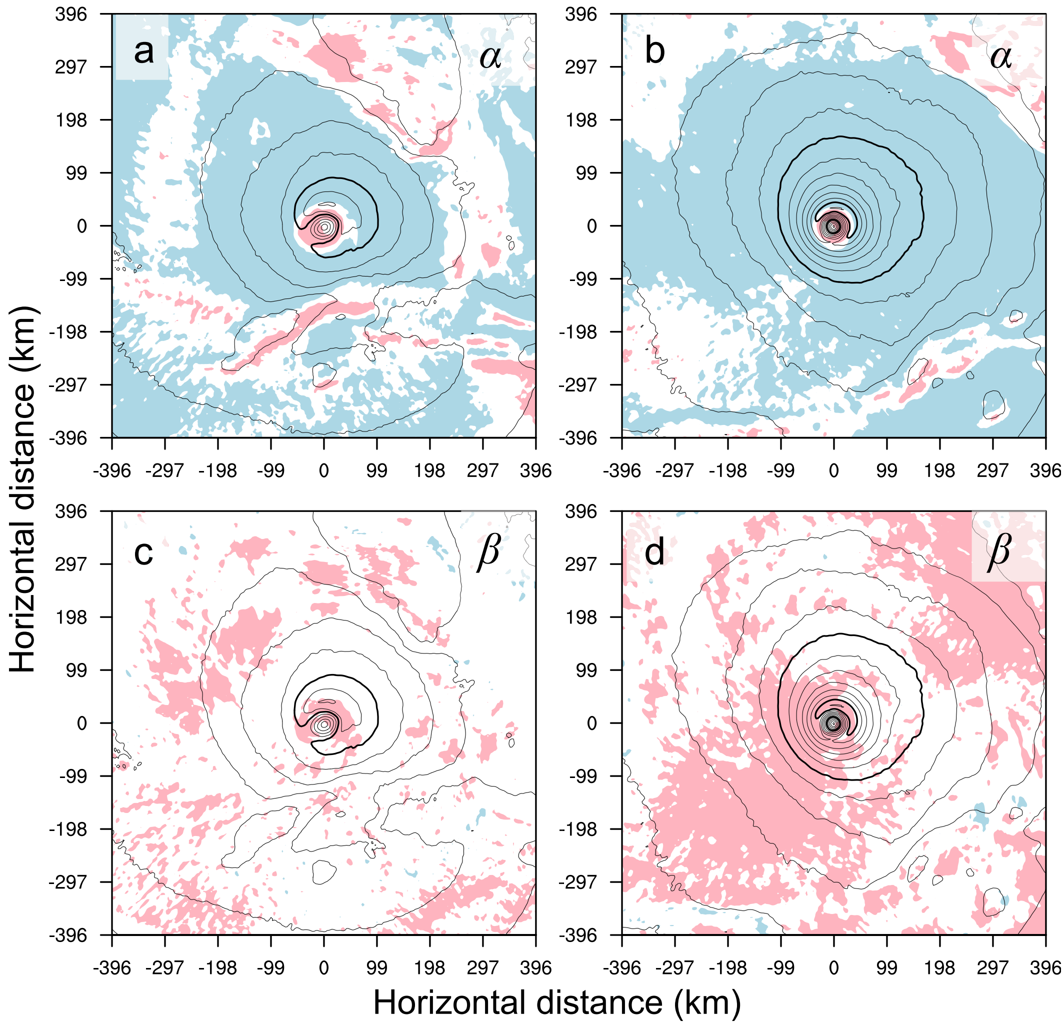

FIG. 11. As in Figs. 9 and 10, but valid 25 h after initialization and in a *vortex-centered* framework (axis labels denote distance in km from the average TC center).

weaker TCs, nonexistent. Thus, the covariance matrix used to update m usually would be sparse and likely contain weak and/or spurious correlations. In contrast, a parameter such as α (with a covariance matrix built off a larger sample size) can be estimated regardless of TC intensity.

Readers may be curious as to why the simulations of Katrina were not compared with the best-track observations, and why the set of model parameters producing the best forecast was not identified. The answer is straightforward: the purpose of this manuscript is not to identify parameter *values* that lead to the best forecast; rather, we seek to identify the parameters most suitable for estimation via EnKF. In fact, using parameter sensitivity to identify optimal parameter values is quite undesirable for several reasons. One, such ‘‘manual tuning’’ is extremely tedious and computationally expensive. Two, the parameter set that produces the best forecast is almost certainly situation dependent, so manual tuning would result in either okay (but not great) forecasts of all TCs or in terrible forecasts for some TCs. Three, manual tuning cannot take advantage of real-time observational data. The EnKF-based parameter estimation, which will be employed in future work, does not have these disadvantages.

So which parameters are most suitable for estimation? In other words, which parameters are *simple*, *observable*, and *distinguishable* based on our sensitivity experiments? As previously noted, simple parameters have ideally linear relationships with state variables. Looking at Figs. 2 and 3, the only parameter that does not exhibit some evidence of simplicity is V_c (no color stratification in Fig. 2 and no statistically significant correlations in Fig. 3). Observability can be identified

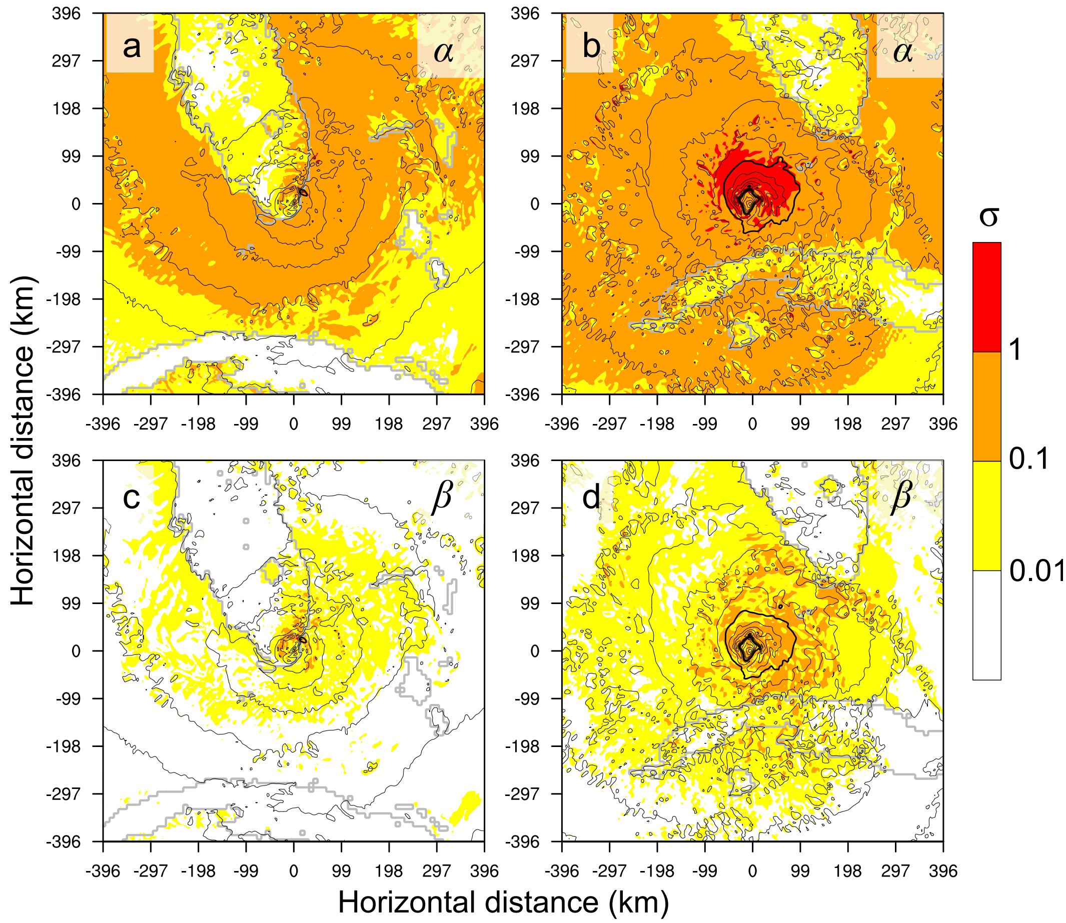

FIG. 12. As in Fig. 9, but for standard deviation of lowest model level wind speed (m s^{-1}, shaded) for *single-parameter* experiments.

through the magnitude of state variable standard deviations from single-parameter experiments. Looking at Fig. 12, α is more observable than β; furthermore, the standard deviations associated with m are only comparable in magnitude to α and β for extremely intense TCs (wind speeds above 60 m s^{-1}, not shown). Also taking into consideration the other problems associated with m (as discussed earlier in this section), it is our contention that m is not suitable for parameter estimation except for very intense storms with abundant observations. The other question is whether α and β are distinguishable from each other. According to Nielsen-Gammon et al. (2010), distinguishable parameters have different correlation structures (i.e., parameters with the same correlation structure are not distinguishable). Even though both α and β can change C_k (Fig. 1), we contend that these two parameters are in fact distinguishable. Plots of the time–radius evolution of correlations between the parameters and surface latent heat flux (Fig. 13) are consistent with the results shown above (cf. Figs. 4 and Figs. 5, 6–11): α and β have distinguishable impacts on the kinematic and thermodynamic structures of the simulated TCs. The key difference between these two parameters is that α (through C_D) affects the pressure–wind relationship, whereas β does not (Figs. 2 and 3).

5. Conclusions

NWP models continue to struggle to accurately forecast TC intensity because many of the important physical processes are parameterized (i.e., they cannot be explicitly resolved by the model). In particular, there is substantial evidence (from theory, observations, and numerical simulations) that fluxes of momentum and moist enthalpy across the air–sea interface have a tremendous effect on TC intensity; unfortunately, air–sea fluxes are extremely difficult to parameterize and thus are likely a significant source of model error. Although the best way to treat model error is still an open research question, an important first step is to be able to quantify

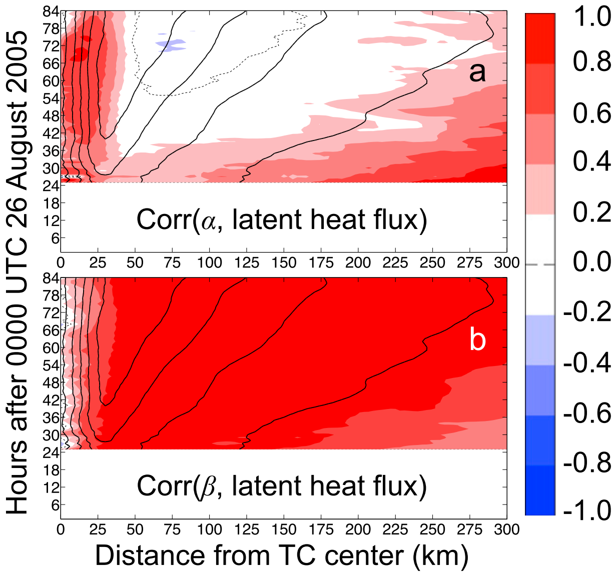

FIG. 13. Hovmöller correlation plots as in Figs. 4 and 5, but for multiparameter simulations initialized at 0000 UTC 27 Aug 2005. (a) Correlations between α and latent heat flux. (b) Correlations between β and latent heat flux.

the effects of model parameters on the forecasted state of the system (i.e., the characteristics of a numerically simulated TC).

This study used ARW-WRF to examine the impacts of four model parameters (three associated with surface drag and one associated with moist enthalpy flux) on simulations of Hurricane Katrina (2005). As expected, surface fluxes had a significant influence on TC intensity and structure. The most straightforward result was that an increase in C_k (the exchange coefficient for moist enthalpy) yielded a more intense TC in terms of both minimum SLP and maximum 10-m wind speed. The finding that C_k does not change the pressure–wind relationship is in agreement with the much less systematic study of Green and Zhang (2013).

This study shows conclusively what was previously noted by Bao et al. (2012) and Green and Zhang (2013): both the pressure–wind relationship and the structure of a TC are affected by changes to C_D (the surface drag coefficient). A somewhat unexpected result is that changes to C_D over *all* wind speeds (as opposed to high wind speeds only) had the most profound impact on the simulated TCs, with higher C_D yielding substantially *lower* minimum SLP (indicative of a stronger storm). A possible explanation for this counterintuitive result is as follows. First, C_k is parameterized to be a function of C_D [cf. (6) and (7)]; therefore, an increase in C_D means an increase in C_k. A direct consequence of an increase in C_k is an increase in the moist enthalpy transferred from the ocean to the overlying air; obviously, more moist enthalpy will result in a deeper TC. By increasing C_D (and thus C_k) at low wind speeds, there is additional moist enthalpy *in the far field* (i.e., well away from the center) that can be advected inward toward the eyewall. This explanation is supported by the fact that when C_D is only allowed to vary at high wind speeds (i.e., in areas close to the eyewall), there is no significant change in minimum SLP. But increased drag will weaken winds farther away from gradient-wind balance, allowing low-level inflow to get closer to TC center (Smith et al. 2013); in other words, increased drag leads to a smaller radius of maximum winds (e.g., Bao et al. 2012; Green and Zhang 2013; Smith et al. 2013).

Additionally, it may be possible to use data assimilation methods to estimate some (but not all) of the model parameters that were tested. The parameters that are most suitable for estimation are α and β, which control the magnitudes of C_D and C_k, respectively, for all wind speeds. Surface wind observations (such as from the Stepped Frequency Microwave Radiometer) and near-surface temperature/moisture data would be most desirable for parameter estimation. The actual parameter estimation experiments are left to a future study.

The functional forms of the equations for C_D and C_k are undoubtedly simplistic (and almost certainly incorrect) because factors such as sea state and radial/azimuthal location with respect to the TC center (e.g., Holthuijsen et al. 2012) are ignored. Broadly speaking, all parameterizations are inherently limited in accuracy because they attempt to represent processes that cannot be explicitly resolved. Nevertheless, sensitivity studies can still provide insight as to how dynamical systems such as TCs respond to parameterized processes and the associated uncertainties (e.g., Emanuel 1986; Bao et al. 2012; Bryan 2012; Smith et al. 2013). Because physical parameterizations are a necessity for NWP, a thorough understanding of their errors and uncertainties can allow for improvements to the forecast—either by changing the parameterization [e.g., Green and Zhang (2013), particularly their Fig. 9] or by incorporating parameter estimation (e.g., Sraj et al. 2013). These approaches by no means replace the need for more physically realistic parameterization schemes developed through theoretical, explicit (resolved) modeling, and/or observational studies.

Finally, it is necessary to point out that the present results are based on an atmospheric model that is not coupled with ocean[8] and wave models. This is particularly

[8] We have done some preliminary tests using a single-column ocean mixing model (Pollard et al. 1972), but the results are beyond the scope of the present paper.

important here because the parameters in question are related to fluxes across the air–sea interface; these fluxes are directly used to couple atmosphere, wave, and ocean models to one another. Therefore, it is likely that the parameter sensitivities (and estimated parameter values) would change with additional parameters, an improved parameterization scheme, and/or a fully coupled model.

Acknowledgments. This material is based upon work supported by a National Science Foundation (NSF) Graduate Research Fellowship under Grants DGE-0750756 and DGE-1255832. Additional support is provided by ONR Grant N000140910526, NSF Grant ATM-0840651, NOAA (HFIP), and the Graduate Visitor Program at the National Center for Atmospheric Research (NCAR). We appreciate the valuable comments provided by Patrick Harr, Jun Zhang, and two anonymous reviewers on earlier versions of the manuscript. We acknowledge high-performance computing (HPC) support from Yellowstone (ark:/85065/d7wd3xhc) provided by NCAR's Computational and Information Systems Laboratory, sponsored by NSF; HPC support was also provided by the Texas Advanced Computing Center (TACC) at the University of Texas at Austin (http://www.tacc.utexas.edu). Discussions with Peter Sullivan, Margaret LeMone, Chris Davis, George Bryan, Wei Wang, Jimy Dudhia, and Daniel Stern were extremely beneficial.

APPENDIX A

Atmospheric Surface Layer

a. Fluxes

The fluxes of momentum τ, sensible heat H, and latent heat E across the atmospheric surface layer are

$$\tau = -\rho u_*^2 = -\rho C_D (\Delta U)^2 = -\rho C_D U^2, \quad \text{(A1)}$$

$$H = -\rho c_p u_* \theta_* = -(\rho c_p) C_H U \Delta\theta, \quad \text{and} \quad \text{(A2)}$$

$$E = -\rho L_v u_* q_* = -(\rho L_v) C_Q U \Delta q, \quad \text{(A3)}$$

where ρ is the density of air; u_* is the friction velocity; θ_* and q_* are the surface layer temperature and moisture scales, respectively; $\Delta(U, \theta, q)$ are the respective differences in wind speed, temperature, and water vapor between a reference height z_{ref} (often 10 m) and the bottom of the surface layer (note that $U = 0$ at the bottom of the surface layer); c_p is the specific heat capacity of air; L_v is the enthalpy of vaporization; and C_D, C_H, and C_Q are the respective bulk exchange coefficients for drag, sensible heat, and latent heat, respectively.

Monin–Obukhov similarity theory may be used to calculate u_*, θ_*, and q_*:

$$u_* = \frac{kU}{\ln\left(\frac{z_{\text{ref}}}{z_0}\right) - \psi_m\left(\frac{z_{\text{ref}}}{L_0}\right)}, \quad \text{(A4)}$$

$$\theta_* = \frac{k\Delta\theta}{\ln\left(\frac{z_{\text{ref}}}{z_0}\right) + \ln\left(\frac{z_0}{z_T}\right) - \psi_h\left(\frac{z_{\text{ref}}}{L_0}\right)}, \quad \text{and} \quad \text{(A5)}$$

$$q_* = \frac{k\Delta q}{\ln\left(\frac{z_{\text{ref}}}{z_0}\right) + \ln\left(\frac{z_0}{z_Q}\right) - \psi_h\left(\frac{z_{\text{ref}}}{L_0}\right)}, \quad \text{(A6)}$$

where k is the von Kármán constant; z_0, z_T, and z_Q are the roughness lengths for momentum, sensible heat, and water vapor (latent heat), respectively; ψ_m and ψ_h are the stability correction functions for momentum and heat, respectively; and $L_0 = u_*^2\theta_0(kg\theta_*)^{-1}$, where g is the acceleration due to gravity and θ_0 is the base-state temperature. In neutral stability,

$$\psi_m\left(\frac{z_{\text{ref}}}{L_0}\right) = \psi_h\left(\frac{z_{\text{ref}}}{L_0}\right) = 0. \quad \text{(A7)}$$

Observations suggest a neutrally stable surface layer within the TC eyewall (e.g., Powell et al. 2003). Therefore, we can use (A7) in (A4)–(A6) to get

$$u_* = \frac{kU}{\ln\left(\frac{z_{\text{ref}}}{z_0}\right)}, \quad \text{(A8)}$$

$$\theta_* = \frac{k\Delta\theta}{\ln\left(\frac{z_{\text{ref}}}{z_0}\right) + \ln\left(\frac{z_0}{z_T}\right)} = \frac{k\Delta\theta}{\ln\left(\frac{z_{\text{ref}}}{z_T}\right)}, \quad \text{and} \quad \text{(A9)}$$

$$q_* = \frac{k\Delta q}{\ln\left(\frac{z_{\text{ref}}}{z_0}\right) + \ln\left(\frac{z_0}{z_Q}\right)} = \frac{k\Delta q}{\ln\left(\frac{z_{\text{ref}}}{z_Q}\right)}. \quad \text{(A10)}$$

b. Exchange coefficients

We can combine (A1)–(A3) with (A8)–(A10) to find expressions for the bulk exchange coefficients (assuming neutral stability, as denoted by the subscript N):

$$C_{D,N} = \frac{k^2}{\left[\ln\left(\frac{z_{\text{ref}}}{z_0}\right)\right]^2}, \quad \text{(A11)}$$

$$C_{H,N} = \frac{k^2}{\ln\left(\frac{z_{\rm ref}}{z_0}\right) \times \ln\left(\frac{z_{\rm ref}}{z_T}\right)} = \frac{C_{D,N}^{1/2} k}{\ln\left(\frac{z_{\rm ref}}{z_T}\right)}, \quad \text{and} \tag{A12}$$

$$C_{Q,N} = \frac{k^2}{\ln\left(\frac{z_{\rm ref}}{z_0}\right) \times \ln\left(\frac{z_{\rm ref}}{z_Q}\right)} = \frac{C_{D,N}^{1/2} k}{\ln\left(\frac{z_{\rm ref}}{z_Q}\right)}. \tag{A13}$$

APPENDIX B

Potential Intensity Theory

Complete formulas

As stated in section 2, the nondimensional forms of the potential intensity theory equations for $V_{\max}$ and $P_{\min}$ are given by Emanuel (1995a,b) as follows:

$$V_{\max}^2 = \frac{C_k}{C_D}\left(\frac{1 - 0.25r_0^2}{1 - \frac{\gamma}{2}\frac{C_k}{C_D}}\right) \quad \text{and} \tag{B1}$$

$$P_{\min} \approx -\frac{V_{\max}^2(1 - 0.5AH) - 0.25r_0^2}{1 - AH}, \tag{B2}$$

with

$$\gamma \equiv A\left(\frac{1 - H}{1 - AH}\right) \quad \text{and} \tag{B3}$$

$$A \equiv \frac{T_s - T_o}{T_s} + \frac{\chi_s}{R_d T_s (1 - H)}, \tag{B4}$$

where C_k and C_D are the surface exchange coefficients of moist enthalpy and drag (momentum), respectively; r_0 is the (normalized) outer radius of the TC at which the surface wind vanishes; H is the ambient relative humidity; T_s and T_o are the surface and outflow temperatures, respectively; χ_s is the background entropy deficit (with respect to the ocean) of the subcloud layer; and R_d is the gas constant for dry air.

REFERENCES

Aksoy, A., F. Zhang, and J. W. Nielsen-Gammon, 2006a: Ensemble-based simultaneous state and parameter estimation in a two-dimensional sea-breeze model. *Mon. Wea. Rev.,* **134,** 2951–2970, doi:10.1175/MWR3224.1.

——, ——, and ——, 2006b: Ensemble-based simultaneous state and parameter estimation with MM5. *Geophys. Res. Lett.,* **33,** L12801, doi:10.1029/2006GL026186.

Anderson, J. L., 2001: An ensemble adjustment Kalman filter for data assimilation. *Mon. Wea. Rev.,* **129,** 2884–2903, doi:10.1175/1520-0493(2001)129<2884:AEAKFF>2.0.CO;2.

Bao, J.-W., S. A. Michelson, and J. M. Wilczak, 2002: Sensitivity of numerical simulations to parameterizations of roughness for surface heat fluxes at high winds over the sea. *Mon. Wea. Rev.,* **130,** 1926–1932, doi:10.1175/1520-0493(2002)130<1926:SONSTP>2.0.CO;2.

——, S. G. Gopalakrishnan, S. A. Michelson, F. D. Marks, and M. T. Montgomery, 2012: Impact of physics representations in the HWRFX model on simulated hurricane structure and wind–pressure relationships. *Mon. Wea. Rev.,* **140,** 3278–3299, doi:10.1175/MWR-D-11-00332.1.

Black, P. G., and Coauthors, 2007: Air–sea exchange in hurricanes: Synthesis of observations from the Coupled Boundary Layer Air–Sea Transfer Experiment. *Bull. Amer. Meteor. Soc.,* **88,** 357–374, doi:10.1175/BAMS-88-3-357.

Bleck, R., 2002: An oceanic general circulation model framed in hybrid isopycnic-Cartesian coordinates. *Ocean Modell.,* **4,** 55–88, doi:10.1016/S1463-5003(01)00012-9.

Braun, S. A., and W.-K. Tao, 2000: Sensitivity of high-resolution simulations of Hurricane Bob (1991) to planetary boundary layer parameterizations. *Mon. Wea. Rev.,* **128,** 3941–3961, doi:10.1175/1520-0493(2000)129<3941:SOHRSO>2.0.CO;2.

Brutsaert, W., 1975: A theory for local evaporation (or heat transfer) from rough and smooth surfaces at ground level. *Water Resour. Res.,* **11,** 543–550, doi:10.1029/WR011i004p00543.

Bryan, G. H., 2012: Effects of surface exchange coefficients and turbulence length scales on the intensity and structure of numerically simulated hurricanes. *Mon. Wea. Rev.,* **140,** 1125–1143, doi:10.1175/MWR-D-11-00231.1.

Charnock, H., 1955: Wind stress on a water surface. *Quart. J. Roy. Meteor. Soc.,* **81,** 639–640, doi:10.1002/qj.49708135027.

DelSole, T., and X. Yang, 2010: State and parameter estimation in stochastic dynamical models. *Physica D,* **239,** 1781–1788, doi:10.1016/j.physd.2010.06.001.

Donelan, M. A., B. K. Haus, N. Reul, W. J. Plant, M. Stiassnie, H. C. Graber, O. B. Brown, and E. S. Saltzman, 2004: On the limiting aerodynamic roughness of the ocean in very strong winds. *Geophys. Res. Lett.,* **31,** L18306, doi:10.1029/2004GL019460.

Dudhia, J., 1989: Numerical study of convection observed during the Winter Monsoon Experiment using a mesoscale two-dimensional model. *J. Atmos. Sci.,* **46,** 3077–3107, doi:10.1175/1520-0469(1989)046<3077:NSOCOD>2.0.CO;2.

Dyson, F., 2004: A meeting with Enrico Fermi. *Nature,* **427,** 297, doi:10.1038/427297a.

Emanuel, K. A., 1986: An air-sea interaction theory for tropical cyclones. Part I: Steady-state maintenance. *J. Atmos. Sci.,* **43,** 585–604, doi:10.1175/1520-0469(1986)043<0585:AASITF>2.0.CO;2.

——, 1995a: The behavior of a simple hurricane model using a convective scheme based on subcloud-layer entropy equilibrium. *J. Atmos. Sci.,* **52,** 3960–3968, doi:10.1175/1520-0469(1995)052<3960:TBOASH>2.0.CO;2.

——, 1995b: Sensitivity of tropical cyclones to surface exchange coefficients and a revised steady-state model incorporating eye dynamics. *J. Atmos. Sci.,* **52,** 3969–3976, doi:10.1175/1520-0469(1995)052<3969:SOTCTS>2.0.CO;2.

French, J. R., W. M. Drennan, J. A. Zhang, and P. G. Black, 2007: Turbulent fluxes in the hurricane boundary layer. Part I: Momentum flux. *J. Atmos. Sci.,* **64,** 1089–1102, doi:10.1175/JAS3887.1.

Garratt, J. R., 1992: *The Atmospheric Boundary Layer.* Cambridge University Press, 316 pp.

Gray, W. M., 1968: Global view of the origin of tropical disturbances and storms. *Mon. Wea. Rev.,* **96,** 669–700, doi:10.1175/1520-0493(1968)096<0669:GVOTOO>2.0.CO;2.

Green, B. W., and F. Zhang, 2013: Impacts of air–sea flux parameterizations on the intensity and structure of tropical cyclones. *Mon. Wea. Rev.,* **141,** 2308–2324, doi:10.1175/MWR-D-12-00274.1.

Grell, G. A., and D. Devenyi, 2002: A generalized approach to parameterizing convection combining ensemble and data assimilation techniques. *Geophys. Res. Lett.,* **29,** 1693, doi:10.1029/2002GL015311.

Holthuijsen, L. H., M. D. Powell, and J. D. Pietrzak, 2012: Wind and waves in extreme hurricanes. *J. Geophys. Res.,* **117,** C09003, doi:10.1029/2012JC007983.

Hong, S.-Y., and J.-O. J. Lim, 2006: The WRF single-moment microphysics scheme (WSM6). *J. Korean Meteor. Soc.,* **42,** 129–151.

——, Y. Noh, and J. Dudhia, 2006: A new vertical diffusion package with an explicit treatment of entrainment processes. *Mon. Wea. Rev.,* **134,** 2318–2341, doi:10.1175/MWR3199.1.

Hu, X.-M., F. Zhang, and J. W. Nielsen-Gammon, 2010: Ensemble-based simultaneous state and parameter estimation for treatment of mesoscale model error: A real-data study. *Geophys. Res. Lett.,* **37,** L08802, doi:10.1029/2010GL043017.

Ito, K., Y. Ishikawa, and T. Awaji, 2010: Specifying air-sea exchange coefficients in the high-wind regime of a mature tropical cyclone by an adjoint data assimilation method. *SOLA,* **6,** 13–16, doi:10.2151/sola.2010-004.

——, T. Kawabata, T. Kato, Y. Honda, Y. Ishikawa, and T. Awaji, 2013: Simultaneous optimization of air-sea exchange coefficients and initial conditions near a tropical cyclone using JNoVA. *J. Meteor. Soc. Japan,* **91,** 337–353, doi:10.2151/jmsj.2013-307.

Jarosz, E., D. A. Mitchell, D. W. Wang, and W. J. Teague, 2007: Bottom-up determination of air-sea momentum exchange under a major tropical cyclone. *Science,* **315,** 1707–1709, doi:10.1126/science.1136466.

Kalnay, E., 2003: *Atmospheric Modeling, Data Assimilation and Predictability.* Cambridge University Press, 341 pp.

Kara, A. B., P. A. Rochford, and H. E. Hurlburt, 2002: Air-sea flux estimates and the 1997-1998 ENSO event. *Bound.-Layer Meteor.,* **103,** 439–458, doi:10.1023/A:1014945408605.

Knabb, R. D., J. R. Rhome, and D. P. Brown, 2006: Tropical cyclone report: Hurricane Katrina 23–30 August 2005. NOAA, 43 pp. [Available online at http://www.nhc.noaa.gov/pdf/TCR-AL122005_Katrina.pdf.]

Mlawer, E. J., S. J. Taubman, P. D. Brown, M. J. Iacono, and S. A. Clough, 1997: Radiative transfer for inhomogeneous atmospheres: RRTM, a validated correlated-k model for the longwave. *J. Geophys. Res.,* **102,** 16 663–16 682, doi:10.1029/97JD00237.

Nielsen-Gammon, J. W., X.-M. Hu, F. Zhang, and J. E. Pleim, 2010: Evaluation of planetary boundary layer scheme sensitivities for the purpose of parameter estimation. *Mon. Wea. Rev.,* **138,** 3400–3417, doi:10.1175/2010MWR3292.1.

Ooyama, K., 1969: Numerical simulation of the life cycle of tropical cyclones. *J. Atmos. Sci.,* **26,** 3–40, doi:10.1175/1520-0469(1969)026<0003:NSOTLC>2.0.CO;2.

Peng, S., Y. Li, and L. Xie, 2013: Adjusting the wind stress drag coefficient in storm surge forecasting using an adjoint technique. *J. Atmos. Oceanic Technol.,* **30,** 590–608, doi:10.1175/JTECH-D-12-00034.1.

Pollard, R. T., P. B. Rhines, and R. O. R. Y. Thompson, 1972: The deepening of the wind-mixed layer. *Geophys. Fluid Dyn.,* **4,** 381–404, doi:10.1080/03091927208236105.

Powell, M. D., P. J. Vickery, and T. A. Reinhold, 2003: Reduced drag coefficient for high wind speeds in tropical cyclones. *Nature,* **422,** 279–283, doi:10.1038/nature01481.

Rappaport, E. N., and Coauthors, 2009: Advances and challenges at the National Hurricane Center. *Wea. Forecasting,* **24,** 395–419, doi:10.1175/2008WAF2222128.1.

Rosenthal, S. L., 1971: The response of a tropical cyclone model to variations in boundary layer parameters, initial conditions, lateral boundary conditions, and domain size. *Mon. Wea. Rev.,* **99,** 767–777, doi:10.1175/1520-0493(1971)099<0767:TROATC>2.3.CO;2.

Saltelli, A., M. Ratto, T. Andres, F. Campolongo, J. Cariboni, D. Gatelli, M. Saisana, and S. Tarantola, 2008: *Global Sensitivity Analysis: The Primer.* Wiley Publishing, 304 pp.

Skamarock, W. C., and Coauthors, 2008: A description of the Advanced Research WRF version 3. NCAR Tech. Note NCAR/TN-475+STR, 113 pp. [Available online at http://www.mmm.ucar.edu/wrf/users/docs/arw_v3_bw.pdf.]

Smith, R. K., M. T. Montgomery, and G. L. Thomsen, 2013: Sensitivity of tropical-cyclone models to the surface drag coefficient in different boundary-layer schemes. *Quart. J. Roy. Meteor. Soc.,* doi:10.1002/qj.2057, in press.

Sraj, I., and Coauthors, 2013: Bayesian inference of drag parameters using Fanapi AXBT data. *Mon. Wea. Rev.,* **141,** 2347–2367, doi:10.1175/MWR-D-12-00228.1.

Vickery, P. J., D. Wadhera, M. D. Powell, and Y. Chen, 2009: A hurricane boundary layer and wind field model for use in engineering applications. *J. Appl. Meteor. Climatol.,* **48,** 381–405, doi:10.1175/2008JAMC1841.1.

Weng, Y., and F. Zhang, 2012: Assimilating airborne Doppler radar observations with an ensemble Kalman filter for convection-permitting hurricane initialization and prediction: Katrina (2005). *Mon. Wea. Rev.,* **140,** 841–859, doi:10.1175/2011MWR3602.1.

Zhang, F., Y. Weng, J. A. Sippel, Z. Meng, and C. H. Bishop, 2009: Cloud-resolving hurricane initialization and prediction through assimilation of Doppler radar observations with an ensemble Kalman filter. *Mon. Wea. Rev.,* **137,** 2105–2125, doi:10.1175/2009MWR2645.1.

Zhang, J. A., P. G. Black, J. R. French, and W. M. Drennan, 2008: First direct measurements of enthalpy flux in the hurricane boundary layer: The CBLAST results. *Geophys. Res. Lett.,* **35,** L14813, doi:10.1029/2008GL034374.

Zupanski, D., and M. Zupanski, 2006: Model error estimation employing an ensemble data assimilation approach. *Mon. Wea. Rev.,* **134,** 1337–1354, doi:10.1175/MWR3125.1.